EXPERIMENTAL STUDY OF GAS-LIQUID-SOLID SLUG FLOW IN HORIZONTAL PIPELINES

Luis M. M. Rosas, mimark777@gmail.com
Fabio A. Schneider, schneider@unibrasil.com.br
Moises A. Marcelino Neto, mneto@utfpr.edu.br
Marco J. Da Silva, mdasilva@utfpr.edu.br
Rigoberto E. M. Morales rmorales@utfpr.edu.pe
Multiphase Flow Research Center (NUEM), Post-graduation Programme in Mechanical and Materials Engineering (PPGEM), Federal University of Technology – Paraná (UTFPR), *Curitiba, PR, Brasil.*
Amadeo Sum, asum@mines.edu
Hydrates Energy Innovation Laboratory, Colorado School of Mines, Golden, CO, USA

Abstract. *Multiphase flows appear during a large number of industrial operations. Such is the case of the offshore oil and gas production operations, where sand or hydrate particles may occasionally be present in the flow. The present work characterizes, on experimental grounds, the gas-liquid-solid three-phase flows in a horizontal pipe. The objective here is to determine the role solid particles (akin to hydrates) play on the characteristic parameters of such flows, namely the bubble front velocity, unit cell frequency and bubble and liquid slug lengths. Experimental tests with liquid-suspended solid particles whose specific masses are similar to those of the hydrate particles were carried out. The test section comprised a 26-mm ID, 9-m long transparent acrylic pipe. The flow structures were monitored and measured by means of resistive sensors and a high-speed camera. Several pairs of gas and liquid superficial velocities at a constant solid particle concentration were investigated during the tests. Standard 0.5-mm polyethylene particles with 938 kg/m^3 of specific mass made the solid phase. The signals captured during the tests were processed and presented in terms of a probability density function (PDF) and averaged values. The experiments and their results are herein discussed and compared with the two-phase gas-liquid flows at similar conditions.*

Keywords*: Experimental study, multiphase flows, gas-liquid-solid, slug flow, solid particles.*

1. INTRODUCTION

Multiphase flows are found in a multitude of industrial processes and applications, and the transportation of hydrocarbon streams is one of them. Therefore, the understanding of those flows is essential to the design of oil and gas production equipment, as well as to assuring their optimal operational performance. In the particular case of hydrocarbon production operations, solid particles such as sand or other sediments are often found. And, depending upon pressure and temperature conditions, hydrates can be formed as well. More recently, the need to evaluate the role played by solid particles on the development of the two-phase gas-liquid flow regime known as slug flow has been identified, as the solids present in the flow might increase the pressure drops and the consequential production rate reduction.

The technical literature reveals a large number of studies on multiphase flows. However, most of those works focus on hydrodynamics aspects of two-phase gas-liquid flows (Wallis, 1969; Dukler e Hubbard, 1975; Fernandez, 1983; Taitel e Barnea, 1990; Taitel e Barnea, 1993; Rodrigues, 2009) or liquid-solid transportation (Davies et al., 1987; Doron et al., 1987; Doron e Barnea, 1993). The existing literature on gas-liquid-solid flows is nevertheless scarce and provides little information about the subject. Those works evaluate the influence of gas-liquid intermittent (slug) flows on particle transportation, and sand is usually the solid suspended matter (Stevenson et al., 2001; Stevenson e Thorpe, 2002, Stevenson e Thorpe, 2003; Gohardeh e Rodgers, 2009; Gohardeh et al. 2009).

The present work studies the influence that solid size and concentration have on the characteristic parameters of gas-liquid slug flows, where solid particles whose specific masses are similar to those pertaining to the hydrate particles were used. The objective here is to analyse the characteristic parameters of the slug flow structures – the bubble front velocity, unit cell frequency and bubble and liquid slug lengths – for different particle concentrations, aiming at comparing them with liquid-gas slug flow parameters. Experimental data will be presented and evaluated by means of the probability density function (PDF) and averaged values.

2. EXPERIMENTAL PROCEDURE

2.1 Experimental Loop

The experimental tests were carried out in an experimental rig in the labs of the Núcleo de Escoamentos Multifásicos (NUEM), a body of the Federal University of Technology (UTFPR). A scheme of the experimental apparatus is shown in Fig. 1. The test section is a 26-mm ID, 9-m long transparent acrylic pipe that allows flow visualization. Two independent air and water-particles feeding lines supply the fluids that will be mixed right before entering the test section. The mixer is at the inlet of the three-phase line. At the end of the test section the mixture is transported to a 310-litre storage tank where the phases are separated by gravity.

A centrifugal pump transports the water-particles mixture/suspension from the reservoir to the flow loop. This Fabo pump model BCIE602/7822 operates with a frequency inverter and a maximum flow rate of 15,000 l/h. A 800-litre air tank is fed by a 2-HP PEG (brand) compressor, both making the air supply skid. Water and particles are mixed before reaching the circuit-feeding centrifugal pump. This water-particles mixing is done by recirculating the water and the particles in the tank by means of another centrifugal pump, thus yielding a homogeneous mixture. The flow rates of the water-particles and air streams are measured by flow meters located at the two feeding lines. The flow rate of the air-water-particles mixture is measured by a Coriolis-type Micromotion flow meter. The air flow rate is measured by 1- and 2-mm orifice plates. Rheotest Haake GMBH rotameters were utilized to calibrate the orifice plates. Air pressure and temperature are also monitored by a differential pressure meter with an incorporated PT100 resistive meter.

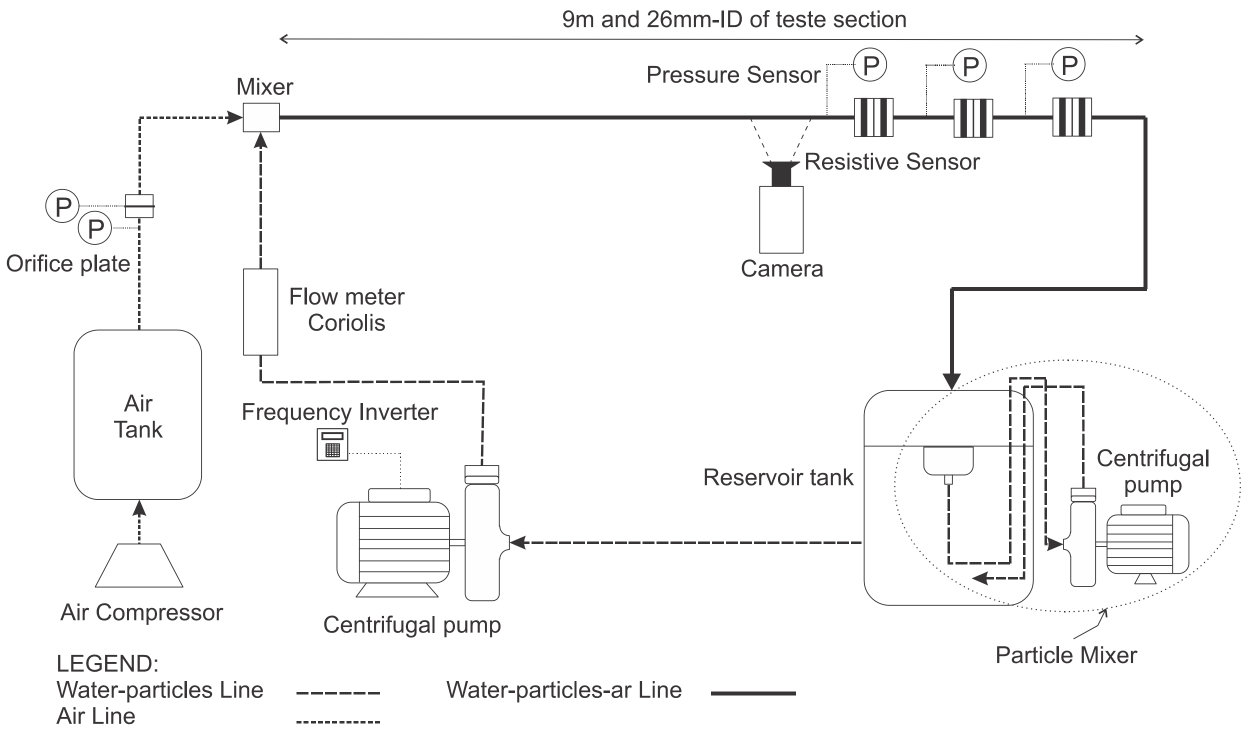

Figure 1. Experimental apparatus

The slug flow structures were monitored through resistive sensors positioned at the end of the test section, so as to capture a fully developed flow and to avoid entrance effects that might affect both the slug flow and the particle suspension. The signal detection times identify the slug flow structures. Thus, the nose and the rear of each bubble are detected, and from the translational velocities the unit cell frequency and both the bubble and liquid slug lengths are computed.

Eq. (1) shows how the superficial velocity of the gas in the test section is computed through the equation of state of an ideal gas. The subscript “0” is relative to the air in the feeding line right before the test section inlet, while the subscript “1” refers to the air in the three-phase test section. “A” is the cross sectional area of the pipe.

$$J_{G1} = \frac{P_1 T_0}{P_0 T_1}\left(\frac{Q_{G0}}{A}\right) \qquad (1)$$

The water superficial velocity in the test section is calculated as a function of the particle concentration, assuming a homogeneous liquid-solid mixture along the pipe as shown by Eq. (2). In this equation, Q_{mix} is the liquid-solid mixture flow rate (given by the Coriolis flow meter), m_{part} and ρ_{part} are, respectively, the mass and the specific mass of the particles and V_{liq} is the total liquid volume.

$$J_L = \frac{Q_{mix}}{A\left(1 + \frac{m_{part}}{\rho_{part} V_{Liq}}\right)} \qquad (2)$$

2.2 Resistive Sensors

The working principle behind this technique was developed by Machado et al. (2013). It is based on the fact that the phases that compose the mixture have different electrical conductivities. Thus, in a two-phase flow, the electrical resistance varies according to the distribution of the phases, and that variation allows the determination of either the phase fractions at a specific cross section of the pipe or the liquid film height, when stratified flow exists.

The resistive sensor is composed of three circuit plates made of fiberglass, with acrylic flanges and O-rings between the plates, as shown in Fig. 2. The central plate is connected to the ground (zero electric potential). That is done to avoid interference of the signals from the other two plates. The plates have two 0.12-mm OD stainless steel wires 3.0 mm apart. The plates work by the emission of a ±5.0 V, 1.75 kHz square signal from one of the wires. The other wire receives the emitted signal, with a strength that depends on the fluids filling the space between the two wires. The maximum tension is reached when the space is completely filled with water and minimum or null when only air fills that gap. During two-phase flows, the voltage fluctuates between those maximum and minimum levels.

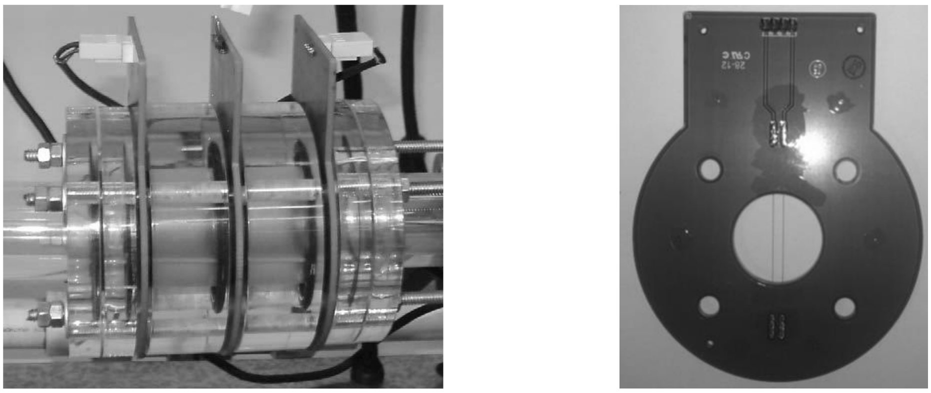

Figure 2. Resistive sensors

3. SIGNAL PROCESSING

The signal processing is based on an algorithm developed by Vicencio (2013). In this algorithm, the void fraction is computed through a linear relationship between the liquid height and the electric tension. Eq. (3) presents such relationship, where *V(t)* is the voltage as a function of time, V_v is the voltage when the liquid completely fills the space between the two wires and V_c is the voltage when only air fills that space. Thence an equation relating the liquid height (h_{LB}) to the gas void fraction (R_G) can be developed, and that is Eq. (4).

$$\frac{h_{LB}}{D} = \frac{V(\text{t}) - V_v}{V_c - V_v} \tag{3}$$

$$R_G = 1 - \frac{1}{\pi}\left(\arccos\left(1 - \frac{2h_{LB}}{D}\right) - \left(1 - \frac{2h_{LB}}{D}\right)\sqrt{1 - \left(1 - \frac{2h_{LB}}{D}\right)^2}\right) \tag{4}$$

Figure 3 shows a void fraction temporal series (after processing) captured by the resistive sensor during an intermittent flow test. A cut factor, represented by a line (FC), is associated to the signals and is used to identify the flow structures. Signals above this line correspond to the elongated bubble, whereas the signals below this line correspond to the liquid slug. A binary function, similar to the one proposed by Bertola (2003), is in charge of the analysis. Cut factors for each temporal series are chosen, depending on the combination of the liquid and gas superficial velocities and from the local aeration. The cut factors range between the maximum and minimum void fraction.

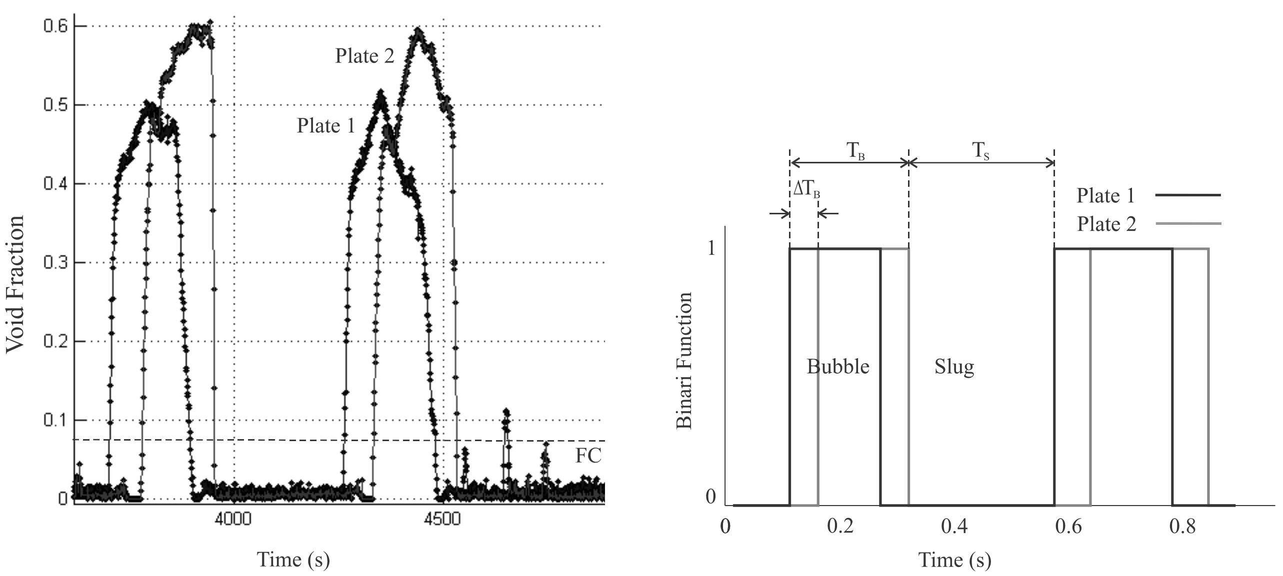

Figure 3. Temporal series for slug flows

Figure 3 shows the binary function associated to the signals for an intermittent flow. T_B and T_S represent, respectively, the travelling time of the bubble and the liquid slug through the sensor. According to Eq. (5), the time lapse in the detection of the elongated bubble front, ΔT_B, is used to compute the elongated bubble front velocity, U_{TB}, since the distance between the two sensor plates, d_S, is known. The bubble and liquid slug lengths are calculated by assuming that the unit cell travels at the elongated bubble front velocity, as per Eqs. (6) and (7). Eq. (8) gives the unit cell frequency.

$$U_{TB} = d_S / \Delta T_B \quad (5)$$

$$L_B = U_{TB} T_B \quad (6)$$

$$L_S = U_{TB} T_S \quad (7)$$

$$f = \frac{1}{T_B + T_S} \quad (8)$$

4. RESULTS

4.1 Test matrix

A test matrix for different mixture velocities (J) within the slug flow region was put together. At those velocities, slug flow should occur throughout the whole test section. Those J-values represent different gas (J_G) and liquid (J_L) superficial velocity pairs. The selected liquid superficial velocities were 0.75, 1.00 and 1.50 m/s, while the gas superficial velocities were 0.5 and 0.75 m/s. Blank tests using the same gas and liquid superficial velocities (but no solid particles) were carried out, for the sake of comparison. In those tests, water and air made the liquid and the gaseous phase, respectively, while 938-kg/m3, 0.5-mm polyethylene particles made the solid phase. A solid particle concentration of 1.0 kg per 250 l of water was used in the tests. Table 1 shows the test matrix.

Table 1. Test matrix

	Particle concentration in the liquid phase						
	0.0 kg/250L				1.0 kg/250L		
PONTO	J_L (m/s)	J_G (m/s)	J (m/s)	PONTO	J_L (m/s)	J_G (m/s)	J (m/s)
P01-0	0.75	0.75	1.50	P01-1	0.75	0.75	1.50
P02-0	1.00	0.50	1.50	P02-1	1.00	0.50	1.50
P03-0	1.50	0.50	2.00	P03-1	1.50	0.50	2.00

Three measurement stations meant to capture the slug flow characteristics were assembled in the test section. Fig. 4. shows those stations.

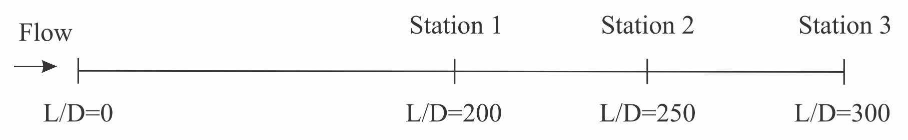

Figure 4. Experimental test section and its measurement stations

4.2 Characteristic parameters of the slug flows

Figure 5 shows experimental PDFs and histograms for points (superficial velocity pairs) P01-1 e P02-1 e P03-1 when solid particles are added to the gas-liquid mixture. With regard to the length of the elongated bubbles (L_B), it has been observed that the probability distributions can be approximated as normal ones. There is a direct relationship between the elongated bubble length and the ratio between the liquid and the mixture flow rates. Therefore, the J_G/J ratio can be used in the analysis of the bubble length. The average L_B values measured at station 3 are shown in Table 3. Thus, for J_G/J = 0.5, the average elongated bubble length is 0.4815 m. For J_G/J = 0.67 the average is 1.2038 m. Finally, for J_G/J = 0.75, the average is 2.2202 m. It becomes therefore clear that the elongated bubble length increases with an increasing J_G/J ratio.

Table 2. Average values of slug flow parameters at measuring station 3.

PONTO	J_G (m/s)	J_L (m/s)	J (m/s)	J_G/J	L_B (m)	L_S (m)	U_{TB} (m/s)	f (Hz)
P01-1	0.75	0.75	1.50	0.50	0.4815	0.2385	2.0592	3.2921
P02-1	1.00	0.50	1.50	0.67	1.2038	0.3404	1.8186	1.3920
P03-1	1.50	0.50	2.00	0.75	2.2202	0.4001	2.6201	1.2170

The liquid slug length, L_S, can be characterized as a log-normal distribution, as observed in Fig. 5. A relationship between L_B and the superficial velocities could not be found in the probability distributions, but as it can be observed the averages have similar values for the same superficial velocities. The averages of the L_S values measured at station 3 are shown in Table 2.

The elongated bubble translational velocity (U_{TB}) can be characterized as a normal distribution. Fig. 5 shows the probability distributions obtained for U_{TB} at station 3. Table 2 shows the average values from the distributions shown in Fig. 5. For the same liquid superficial velocities – e.g. J_L = 0.50 m/s – it can be noted that U_{TB} increases with an increasing J_G. This is consistent with the data shown in Tab. 2, as the elongated bubble velocity increases as long as the mixture velocity also increases.

It was observed that the unit cell frequency (f) behaves as a log-normal distribution. Fig. 5 shows the histograms obtained from the experimental data and their respective tunings. A good agreement between the histograms and their tunings is observed. Table 2 shows the average values and standard deviations the average values and the standard deviations for the frequencies as they are shown in Fig. 5. It can be seen that for a same J_L (J_L = 0.50 m/s) the frequency increases with a decreasing J_G. The same trend had been observed in the other two stations.

An analysis involving two test cases is shown in Fig. 6. The continuous line represents a gas-liquid slug flow case, while the dotted line represents a gas-liquid-solid slug flow case. The term “two-phase” is associated to the gas-liquid flows, whereas “three-phase” describes gas-liquid-solid flows. The PDFs for the slug flow parameters at the three measuring stations are presented for the case P02 (J_G = 1.00 m/s and J_L = 0.50 m/s). The results show a trend for U_{TB}: U_{TB} is always greater in three-phase flows than in two-phase ones, and that is valid for all three stations. This finding is in agreement with the average values observed in Fig. 7. The same trend is observed in all other analysed points, as it can be seen in Fig. 7.

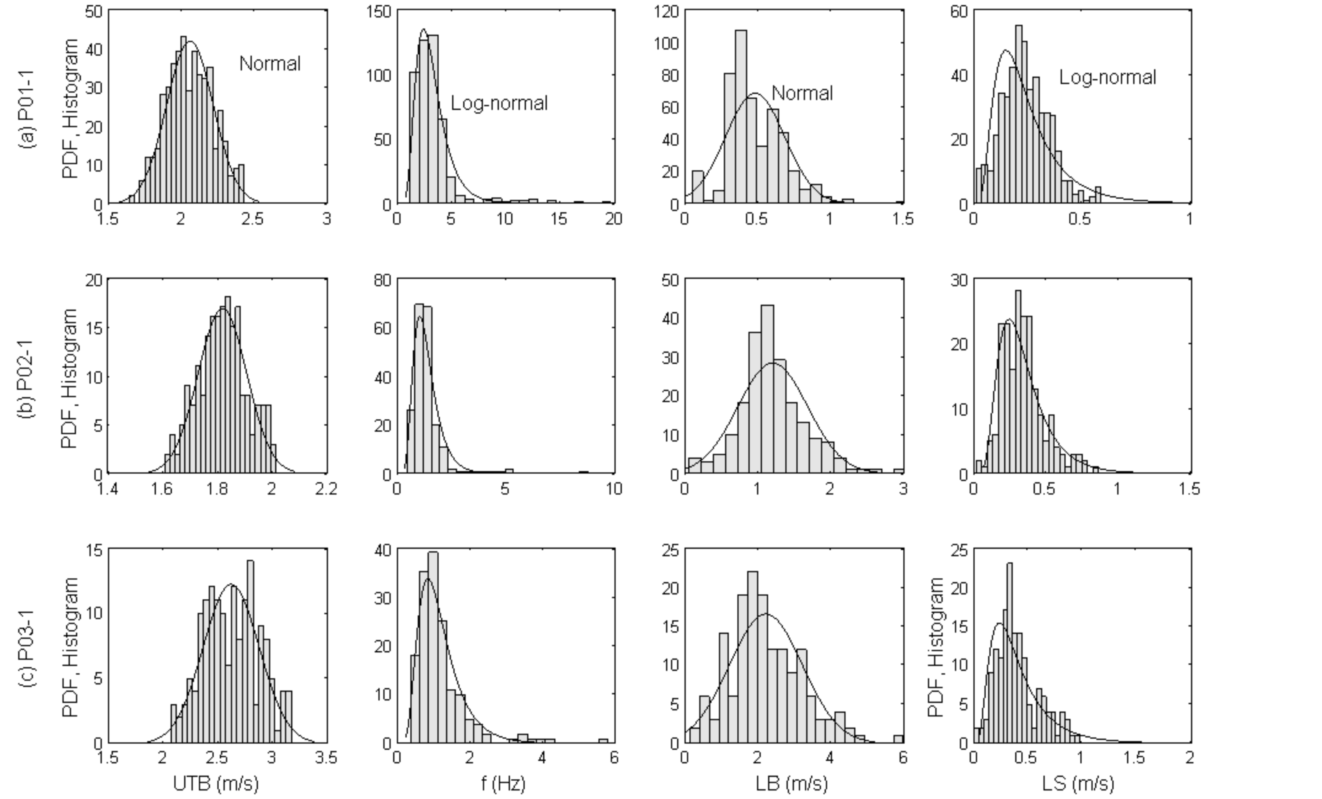

Figure 5. PDFs for flows with solid particles at station 3. (a) P01-1: J_G=0.75m/s and J_L=0.75m/s, (b) P02-1: J_G=1.00m/s and J_L=0.50m/s, (c) P03-1: J_G=1.50m/s and J_L=0.50m/s.

The same trend is observed for the liquid slug length, L_S. The averaged lengths presented in Fig. 7 show a greater value for all the three points when the flow is three-phase. This trend was not observed in the analyses performed for the elongated bubble length, L_B and for the unit cell frequency, *f*.

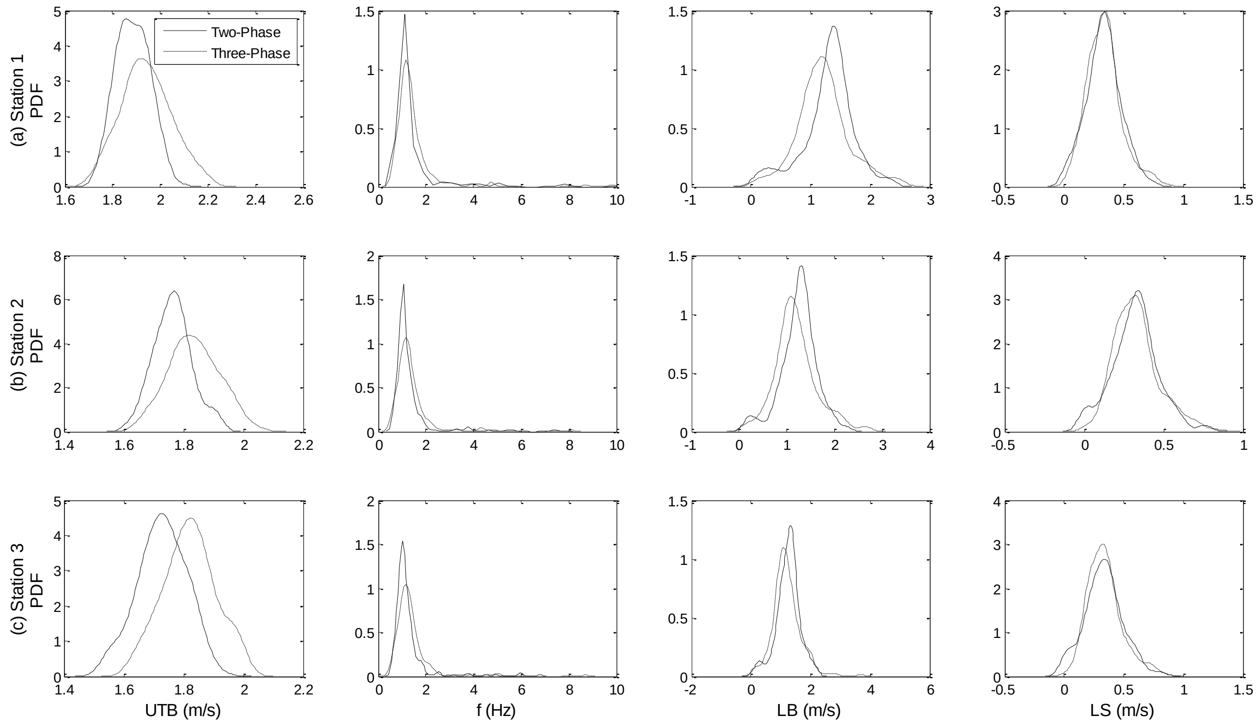

Figure 6. Comparison between PDFs for point P02: J_G= 1.00m/s and J_L= 0.50m/s. a) Station 1. L/D=200, b) Station 2. L/D=250, c) Station 3. L/D=300.

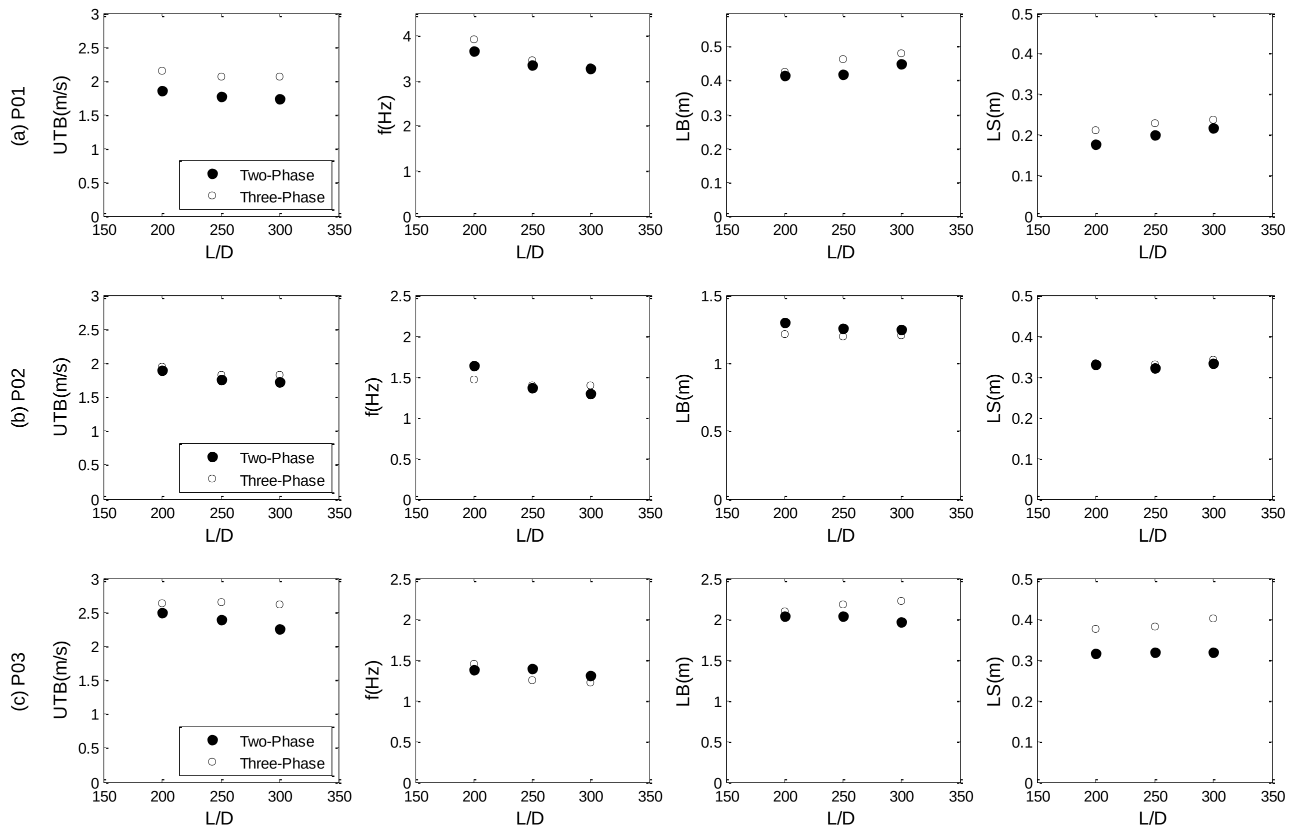

Figure 7. Average parameter values at the three measurement stations. a) P01: J_G = 0.75 m/s and J_L = 0.75 m/s. b) P02: J_G = 1.00 m/s and J_L = 0.50 m/s, c) P03: J_G = 1.50 m/s and J_L = 0.50 m/s.

5. CONCLUSIONS

Experimental analyses on gas-liquid-solid two-phase flows were carried out and their results presented. An experimental rig was built and resistive sensors were used to measure the flow parameters at specific points of the test section. Superficial liquid and gas velocities within the slug flow region were chosen and experimental measurements with and without solid particles were conducted, so as to compare purely two-phase gas-liquid flows with gas-liquid-solid three-phase ones. Probability distributions were computed and normal distributions were found for the elongated bubble velocity and length, whereas the unit cell frequency and the liquid slug length showed a log-normal distribution.

The parameters of slug flows with and without solid particles were compared, and a trend for the elongated bubble translational velocity and the liquid slug length were found: their magnitudes in three-phase gas-liquid-solid slug flows are superior to those found in the purely two-phase gas-liquid ones.

6. REFERENCES

Barnea, D., Taitel, Y. “A model for slug length distribution in gas-liquid slug flow. International Journal of Multiphase Flow”, v. 19, n. 5, p. 829–838, 1993. Elsevier.

Bertola, V. Experimental characterization of gas–liquid intermittent subregimes by phase density function measurements. Experiments in fluids, Springer, v. 34, n. 1, p. 122–129, 2003

Davies, J.T, (1987). Calculation of critical velocities to maintain solids in suspension in horizontal pipes. Vol.42(7), pp.1667-1670, Chemical Engineering Science.

Doron, P., Granica, D. & Barnea, D. (1987), “Slurry flow in a horizontal pipes-experimental and modeling”. Int. J. Multiphase Flow 13, 535-547.

Doron, P. & Barnea, D. (1993), “A three-layer model for solid-liquid flow in horizontal pipes”. Int. J. Multiphase Flow 19, 1029-1043.

Doron, P. & Barnea, D. (1995). “Flow pattern maps for solid-liquid flow in pipes,” Int. J. Multiphase Flow, 22(2), pp. 273-83.

Dukler, A. E., & Hubbard, M. G. (1975). “A model for gas-liquid slug flow in horizontal and nearhorizontal tubes”. Ind. Eng. Chem. Fundam., 14(4), 337-347.

Fagundes, J.R. Netto, J. Fabre, L.M. Peresson, (1999). Shape of long bubbles in horizontal slug flow. Int. J. Multiphase

Flow, 25 (6), pp. 1129–1160.
Fernandes, R. C. (1983). “Hydrodynamic model for gás-liquid slug flow in vertical tubes”. American Institute for Chemical Engineers Journal, 29(6), 981-989.
Goharzadeh, A., Rodgers, P., Touati, C. (2009). “Influence of Gas-Liquid Two-Phase Intermittent Flow on Hydraulic Sand Dune Migration in Horizontal Pipelines,” J. Fluids Eng. 132(7), 071301 (Jun 29, 2010).
Goharzadeh, A., Rodgers, P. (2009). “Experimental characterization of solid particle transport by slug flow using Particle Image Velocimetry”. Journal of Physics: Conference Series, 2009, Vol.147(1), p.012069 (13pp).
Machado, D., Hildebrando, F.; Lipinski, L (2013). Sistema Multicanal de Sensores Resistivos para Medição de Escoamentos Bifásicos. 2013. 64 f. Trabalho de Conclusão de Curso (Engenharia Elétrica) – Departamento Acadêmico de Eletrotécnica, Universidade Tecnológica Federal do Paraná, Curitiba. (In Portuguese).
Oladele, O.B., Kurt, M.R., Catalin, T. (2005). “Particle holdup profile in horizontal gas-liquid-solid multiphase flow pipeline,” Chemical Engineering &Technology, 28(12), pp. 1546-1653.
Ofuchi, Cesar Yutaka. (2011). “Técnicas Avançadas para Análise de Escoamento Bifásico Gás-Líquido em Golfadas.” Universidade Tecnológica Federal do Paraná. (In Portuguese).
Rodrigues, H. (2009). “Simulação númerica do escoamento bifásico gás líquido no padrão de golfadas utilizando um modelo lagrangeano de seguimento de pistões”. Universidade Tecnológica Federal do Paraná, Curitiba. (In Portuguese)
Rosa, E.S. (2004). “Slug flow structure in horizontal slug flow,” Thermal Engineering, 3(2), pp. 151-160.
Stevenson, P., Thorpe, R.B., Kennedy, J.E., McDermott, C. (2001). “The transport of particles at low loading in near-horizontal pipes by intermittent flow,” Chemical Engineering Science, 56, pp. 2149- 2159.
Stevenson, P. & R.B. Thorpe (2002), “The Velocity of Isolated Particles Along a Pipe in Smooth Stratified Gas – Liquid Flow”, AIChE J. 48, 963-969.
Stevenson, P. & Thorpe, R.B. (2003). “Energy dissipation at the slug nose and the modeling of solids transport in intermittent flow,” Canadian Journal of Chemical Engineering, 81(2), pp. 271-278.
Taitel, Y., & Barnea, D. (1990a). “Two phase slug flow. Advances in Heat Transfer”, Harnett J. P. and Irvine Jr. T. F., 20, 83-132.
Taitel, Y., & Barnea, D. (1990b). “A consistent approach for calculating pressure drop in inclined slug flow”. Chemical Engineering Science, 45(5), 199-1206.
Taitel, Y., & Barnea, D. (1998). “Effect of gas compressibility on a slug tracking model”. Chemical Engineering Science", 53(11), 2089-2097.
Turian, R. M. & Yuan, T. F. (1977), “Flow of slurries in pipelines”. AIChE J. 23, 232-243.
Turian, R. M., Hsu, F. L. & Ma, T. W. (1987), “Estimation of the critical velocity in pipeline flow of slurries”. Powder Technol. 51, 35-47.
Vicencio, F. E. C. (2013). Caracterização experimental do escoamento intermitente líquido-gás em tubulações horizontais. Dissertação (Mestrado) — Programa de Pós Graduação em Engenharia Mecânica e de Materiais, UTFPR. (In Portuguese).
Wallis, G. B. (1969). “One dimensional-two-phase flow. New York: McGraw-Hill”.

7. RESPONSIBILITY NOTICE

The authors are the only responsible for the printed material included in this paper.